Ciprofloxacin HCl and quercetin functionalized electrospun nanofiber membrane : fabrication and its evaluation in full thickness wound healing

Ajmal, Gufran; Bonde, Gunjan Vasant; Thokala, Sathish; Mittal, Pooja; Khan, Gayasuddin; Singh, Juhi; Pandey, Vivek Kumar; Mishra, Brahmeshwar

2019

https://hdl.handle.net/10356/145327

https://doi.org/10.1080/21691401.2018.1548475

Taylor & Francis
Taylor & Francis Group

Ciprofloxacin HCl and quercetin functionalized electrospun nanofiber membrane: fabrication and its evaluation in full thickness wound healing

Gufran Ajmal[a] , Gunjan Vasant Bonde[a] , Sathish Thokala[a] , Pooja Mittal[a] , Gayasuddin Khan[a], Juhi Singh[a,b] , Vivek Kumar Pandey[c] and Brahmeshwar Mishra[a]

[a]Department of Pharmaceutical Engineering & Technology, Indian Institute of Technology (BHU), Varanasi, India; [b]Interdisciplinary Graduate School, Nanyang Technological University, Singapore, Singapore; [c]Department of Chemical Engineering & Technology, Indian Institute of Technology (BHU), Varanasi, India

ABSTRACT

Microbial infection and oxidative damage of the fibroblast often results in prolonged and incomplete wound healing. Therefore, there is an increasing demand for a scaffold being effective to prevent any possible infection and neutralize excessively released free radicals. Herein, we designed a PCL-based nanofiber loaded with ciprofloxacin hydrochloride (CHL) and quercetin. Developed nanofiber showed the formation of smooth and continuous nanofiber with 101.59 ± 29.18 nm average diameter and entrapping the drugs in amorphous form without any possible physico-chemical interaction between drugs and excipient. High entrapment efficiency (CHL: 92.04% and Que: 94.32%) and prolonged in-vitro release (for 7 days) demonstrated the capability of scaffold to suppress any probable infection and oxidative damage, which was further confirmed by in-vitro antibacterial and antioxidant activity. The biocompatibility of scaffold for direct application to wound site was evaluated through hemocompatibility and cytocompatibility assay. The wound healing efficacies of nanofiber were assessed using full thickness wound model in rats, which displayed accelerated wound healing with complete re-epithelialization and improved collagen deposition within 16 days. In-vivo wound healing finding was further corroborated by SOD, catalase, and hydroxyproline assay. The current study validates the application of ciprofloxacin HCl and quercetin functionalized nanofiber as a potential wound dressing material.

Introduction

The loss of protective function of skin due to severe disease or trauma (physical, chemical, thermal or microbial) is known as a wound [1,2]. Depending on the depth of the skin layer, a wound can be either confined to epidermal layer, which heals via re-epithelialization without any skin graft or due to loss of both epidermis and dermis, i.e., full thickness wounds (FTW). The consequence of FTW is the loss of residual cells for regeneration except for the peripheral region of the wound area. In such situation, complete re-epithelialization of skin either takes longer duration, which often results into scarring of bases and significant disability or it demands skin regeneration product for prompt wound healing [3,4]. Although split-thickness skin graft is usually implanted to promote early wound healing, however its application is restricted by donor sites availability, cumbersome surgical procedures and a tendency to contact with time [5,6]. These limitations lead

the way towards the development of engineered matrices for the skin graft.

Wound healing is a complicated process. The ideal healing progresses through haemostasis, inflammation, proliferation, and tissue remodelling phase with varying and overlapping phase duration. Among those phases, the inflammatory phase is the most critical one during which neutrophils release reactive oxygen species (ROS), reactive nitrogen species (RNS), peroxides and proteases. The major problem associated with open FTW is vulnerability to microbial infections, which activate the body's immune system and aggravate neutrophils' release. In such situation, even endogenous anti-oxidants like superoxide dismutase (SOD), catalase, and glutathione, which make the first line defence mechanism against free radicals, fails to neutralize it. Consequently, these excess free radicals cause oxidative damage to the fibroblast, primary cell responsible for collagen synthesis and provisional extracellular matrix (ECM) formation [7,8]. However, this

problem can be mitigated by enriching the wound site with an external anti-oxidant and antimicrobial drug. Therefore, we have proposed to develop a poly (ε-caprolactone) based nanofiber membrane functionalized with a combination of an antimicrobial and an anti-oxidant for accelerated wound healing.

Recently, electrospinning has gained widespread attention for fabricating nanofibrous scaffold over other techniques as melt-blown, wet-spinning, self-assembly, lithography, etc., because of its comparatively simple, adaptable, cost-effective setup, and ease of scale-up system. [9,10]. Nanofiber developed by electrospinning technique offer several potential advantages for wound healing such as (i) high surface to volume ratio, (ii) highly porous scaffold, (iii) a morphological and structural similarity with natural ECM, (iv) protection of wound from bacterial infiltration owing to highly interconnected pores, (v) a local drug delivery device with high drug loading, sustained and controlled release profile [3,5,11,12].

Numerous high molecular weight polymers have been explored for the production of nanofibers by electrospinning. Poly (ε-caprolactone) (PCL) is one of the extensively examined, and USFDA approved polymer for controlled drug delivery. Biodegradable, bioresorbable, biocompatible and sound mechanical properties of PCL find its significant use for medical and drug delivery devices. Chemical compatible nature of PCL with a wide range of drugs and slow degradation rate paved the way for designing the controlled and sustained delivery device [3,11]. Comparatively low cost of PCL along with mentioned properties render it a suitable candidate for biomedical applications.

Ciprofloxacin hydrochloride (CHL) is a most commonly used fluoroquinolone antibiotic for a variety of local bacterial infections, such as ear, nose, eye, skin, etc. Low minimal inhibitory concentration value against both Gram-negative and positive microorganism and lower frequency of microbial resistance makes it a promising antimicrobial for wound infection [13–15]. Quercetin (Que) is a naturally occurring flavonoid, commonly found in fruits and vegetables. High propensity for electron transfers proves it as strong free radical scavenger and potential anti-oxidant. Additionally, it also shows other health-beneficial effect like anti-carcinogenic, antiviral, anti-allergic and anti-inflammatory properties [16–18].

In this study, PCL based nanofiber functionalized with ciprofloxacin HCl and quercetin was prepared by electrospinning. We hypothesized that; fabricated nanofiber having morphological similarity with natural ECM could progress wound closure and skin regeneration in open FTW. We evaluated this assumption in a rat model and found that PCL/CHL/Que nanofiber effectively reduced any possible infection and promoted collagen synthesis by preventing the oxidative damage of fibroblast.

Materials and methods

Electrospinning of nanofibers

The materials used in the present work are given in **S1**. Electrospinning solutions of different compositions were prepared in acetic acid : formic acid (AA:FA = 7:3 v/v) solvent mixture as per the scheme given in Table 1. Although acetic acid is an independent solvent for PCL and CHL dissolution, owing to the medium dielectric constant (6.2 at 25 °C) and poor electric conductivity, it is not suitable for electrospinning. Mixing it with formic acid (high dielectric constant solvent, 57.9 at 25 °C) facilitates the electrospinning process. Dimethyl sulfoxide was used as co-solvent for solubilization of quercetin. The final solution was filled in a 5 mL syringe fitted with a 24 G needle and was maintained at 8–10 cm distance from the collector. The electrospinning solution was pumped at a flow-rate 0.6 mL/h from the syringe and electrospun at a voltage of 16 kV. All the experiments were performed at ambient room condition (temperature = 24 °C; relative humidity = 65 ± 5%). Steps involved in electrospinning are shown in Figure 1.

Characterization of nanofiber membrane

Morphological study

Nanofiber diameter and porosity were determined using high-resolution scanning electron microscopy

Table 1. Fibre morphology, average diameter, porosity and entrapment efficiency of nanofiber membrane of different compositions.

Sample	PCL (%w/v)	CHL (%w/w of PCL)	Que (%w/w of PCL)	Fibre Morphology	Average Diameter (nm)	Membrane Porosity (%)	Entrapment Efficiency (%)
F1	8	0	0	Beaded Nanofibers	60.35 ± 27.78	80.35%	–
F2	12	0	0	Bead-free, semi-continuous Nanofibers	79.07 ± 22.49	78.56%	–
F3	12	10	0	Bead-free, continuous, lateral perturbation	126.11 ± 33.57	72.70%	CHL: 91.56
F4	12	10	5	Bead-free, continuous, a few lateral perturbation	101.59 ± 29.18	69.36%	CHL: 92.04 Que: 94.32

F2, F3, and F4 were chosen for further studies.
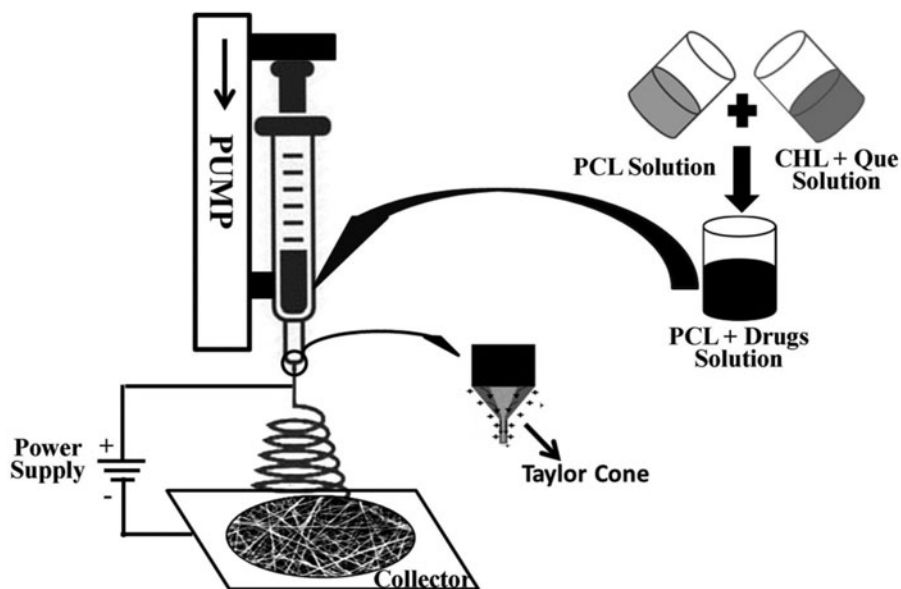The data are expressed as means ± SD, $n = 3$.

Figure 1. Graphic demonstration of steps involved in the electrospun nanofiber mat production.

(HR-SEM) (FEI, Quanta 200 F, Japan). The three dimensional morphology was performed by Atomic Force Microscopy (NTEGRA Prima, NT-MDT, Russia) (refer S2).

Solid-state characterizations

Fourier transform infrared (FTIR) and powder X-ray diffraction (XRD) analyses were done to examine the any possible drugs interaction and change in crystalline property of the drugs encapsulated in nanofiber film (refer S3).

Drug entrapment efficiency and in-vitro release profile

The amount of drugs entrapped in nanofiber was quantified spectrophotometrically (UV-1800 UV-Vis Spectrophotometer, Shimadzu) by simultaneous equation methods. In-vitro drug release characteristics of developed PCL/CHL/Que-nanofiber membrane were determined in phosphate buffer saline (PBS; pH 7.4) (refer S4).

In-vitro antioxidant activity

2,2-diphenyl-1-picrylhydrazyl (DPPH) scavenging efficacies were used to examine the in-vitro antioxidant activity of nanofiber membrane. Antioxidant activity were performed by two methods, i.e., 'Fixed reaction time' and 'Time-dependent assay' [8,19]. In case of 'Fixed reaction time' method, 5 mg electrospun films were added in 3 mL DPPH ethanolic solution (100 μM) and incubated in the dark condition for 0.5 h. After that, the decrease in absorbance was measured

spectrophotometrically at 517 nm. Following equation was used to calculate DPPH scavenging activity:

$$\text{DPPH scavenging } (\%) = \left(\frac{A_0 - A_S}{A_0} \right) \times 100 \qquad (1)$$

where, A_0 and A_s denotes the absorbance at 517 nm of DPPH solution in the absence and presence of electrospun film, respectively.

For 'time-dependent antioxidant assay' of PCL/CHL/Que nanofiber, a series of nanofiber suspension (5 mg in 1 mL PBS buffer) was prepared for the different time interval. At fixed time, the suspension was incubated with 1 mL DPPH solution for 0.5 h, subsequently; the absorbance was recorded at 517 nm.

In-vitro antibacterial activity

Antimicrobial efficacy of prepared nanofiber films were assessed against Gram-positive *Staphylococcus aureus* (MTCC1303) using film diffusion method [14]. The microorganism was pre-cultured overnight in Luria–Bertani medium in a rotary shaker at 37 ± 1 °C. Subsequently, broth was centrifuged at 12,000 rpm for 3 min, resulting pellet was re-suspended and diluted to obtain a standard working suspension (10^8 cells/mL). The 100 μL of standard working bacterial suspension was spread on nutrient agar plate surface using sterile swab sticks. Thereafter, nanofiber films of 5 mm diameter were placed on an agar plate surface and incubated at 37 ± 1 °C for 24 h. After every 24 h, films were shifted to another fresh agar plate seeded with *S.*

aureus, and the zones of inhibitions were determined on days 1, 3, 5 and 7.

Biocompatibility assay

Hemocompatibility of nanofiber membrane

Haemolytic property of nanofiber films was determined by following previously reported method [20]. 2 mL of human blood was centrifuged at 4500 rpm for 10 min at room temperature to separate out plasma. Settled erythrocyte pellet was re-suspended in an equal volume of normal saline (0.9%) by mixing gently. The obtained erythrocyte suspension was centrifuged again to remove any traces of plasma. This washing procedure was repeated thrice. Finally, the erythrocytes were re-suspended into a 2 mL normal saline solution to obtain a working solution. 5 mg of each nanofiber film was mixed with 1 mL of erythrocyte working suspension separately. Negative control and positive control samples (100% lysed erythrocyte) were prepared by mixing equal volumes of erythrocyte working suspension with normal saline and 1% Triton X-100, respectively. All samples were incubated at 37 °C for 30 min. Subsequently, the samples were centrifuged at 4500 rpm for 10 min to settle down intact RBCs. The supernatant (150 μL) was incubated for 20 min at room temperature to allow the oxidation of haemoglobin into oxy-haemoglobin. The UV-absorbance of oxy-haemoglobin was measured at 540 nm. The percentage of erythrocyte haemolysis was determined using following equation:

$$Hemolysis\ (\%) = \left(\frac{A_{sample} - A_{negative\ control}}{A_{positive\ control} - A_{negative\ control}} \right) \times 100$$

(2)

Whereas A_{sample}, $A_{negative\ control}$ and $A_{positive\ control}$ denote the absorbance of test sample, negative control and positive control, respectively.

Cytocompatibility of nanofiber membrane

Cytocompatibility of nanofibers was screened by MTT assay (3-[4,5-dimethylthiazol-2-yl]-2,5-diphenyltetrazolium bromide) against mouse fibroblast cell lines (3T6-Swiss albino). The pre-sterilized samples were incubated in Dulbecco's modified eagle medium (DMEM) at 2 cm^2/mL of media at 37 °C for 24 h to get the extract of the samples. 100 μL of cell lines (at a density 1×10^4/mL) in DMEM medium (supplemented with 10% v/v foetal bovine serum) was pipetted out into 96-well microtitre plate and incubated at 37 °C for 24 h under 5% CO_2 environment. After incubation, extracted samples (100 μL/well) were added in the culture medium and incubated for three-time point, i.e., 24 h, 48 h, 72 h. At the end of incubation time, respective samples were treated with 10 μL/well MTT (10 mg/mL in PBS solution) and further incubated for 4 h under the same condition. Afterward, culture medium and MTT was removed, and dimethyl sulphoxide (200 μL/well) was added to dissolve the insoluble formazan crystal into a purple coloured solution. After shaking the plate for 10 min, the absorbance was measured with a multimode reader at 570 nm wavelength. The following equation determined the percentage cell viability:

$$Cell\ Viability\ (\%) = \left(\frac{A_{sample} - A_{nagative\ control}}{A_{positive\ control} - A_{negative\ control}} \right) \times 100$$

(3)

where, A_{sample}, $A_{positive\ control}$ and $A_{negative\ control}$ denotes the absorbance of culture medium treated with nanofibers extract, untreated cell culture medium and DMSO, respectively.

In-vivo *wound healing study*

Circular-excision wound model was employed to study the wound wrinkling and contracting time. All the experimental protocol was pre-approved by the Central Animal Ethical Committee (CAEC) of Banaras Hindu University, Varanasi (No. Dean/2018/CAEC/638). 24 healthy adult male Wistar rats (200–250 g) were anesthetized separately by an intraperitoneal injection of xylazine (5 mg/kg) and ketamine (35 mg/kg). The dorsal surface of animals was shaved carefully and sterilized with ethanol (70% v/v in water), and a full thickness circular wound (2.5 cm diameter) was made by excising the skin up to the level of subcutaneous panniculus carnosus. Animals were distributed into four groups ($n = 6$). Group-1 was covered with gauze, group-2, group-3, and group-4 were treated with PCL, PCL/CHL, and PCL/CHL/Que-nanofiber membrane respectively. On regular interval post-surgery, wounds were snapped and the size of wound was outlined using a tracing paper, obtained wound boundary was traced back on a graph paper (2 mm^2) and wound area was calculated. The following equation determined the percentage of wound closure:

$$Wound\ closure\ (\%) = \left(\frac{A_0 - A_t}{A_0} \right) \times 100$$

(4)

A_0 is wound area at day 0 and A_t is wound area on day 4, 8, 12 and 16 post surgery.

Then, on post-surgery days 8 and 16, granulation tissue from healed area was harvested and divided into

three portions. The first portion was preserved in formalin (10% v/v in neutral buffer) for further evaluation of histological alteration. The second portion was rinsed with ice-cold saline, homogenized in ice-cold potassium phosphate buffer (pH 7.4, 50 mM). The tissue homogenates were centrifuged for 25 min at 5000 rpm at 5 °C, and supernatants were collected for endogenous antioxidant analysis in granulation tissue [21]. The third portion was acid hydrolyzed for hydroxyproline content analysis.

Histological examination

Granulation tissues preserved into formalin were embedded in paraffin, cut into 5 μm thick section and stained with haematoxylin − eosin (H&E). Histological changes were qualitatively observed under the optical microscope.

Antioxidant enzyme assay

Superoxide free radical scavenging activity of SOD was determined in the tissue supernatant as per the method described by Beauchamp and Fridovich [22] and modified by Ak and Gülçin [23]. Superoxide free radicals were produced in riboflavin/methionine/EDTA/irradiate system and quantitatively evaluated by the reduction of NBT to form colour product (blue formazan), which was measured spectrophotometrically at 560 nm. When SOD containing supernatant was added in the above solution, SOD started scavenging the superoxide, thereby inhibiting the reduction of NBT. The reduced absorbance of the reaction mixture indicates improved superoxide scavenging activity. A reaction mixture devoid of SOD served as control. The superoxide radical scavenging activity was calculated by using the following equation:

$$Superoxide\ radical\ scavenging\ activity\ (\%) = \left(\frac{A_C - A_S}{A_C}\right) \times 100$$

$$(5)$$

where, A_C denotes the absorbance of the reaction mixture without tissue supernatant, and A_S is the absorbance of the reaction mixture with tissue supernatant. The activity of SOD was expressed as Unit/mg
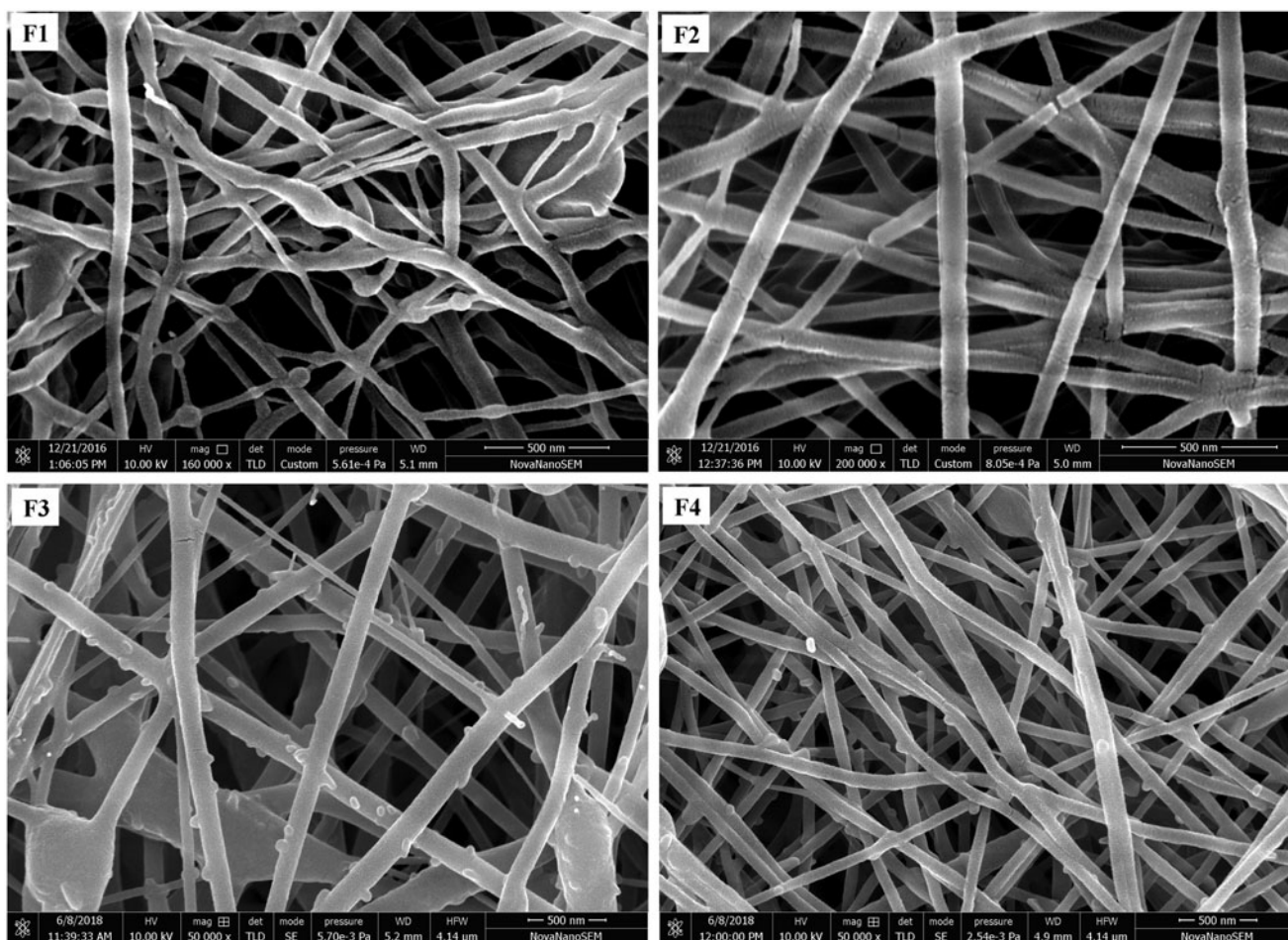

Figure 2. HR-SEM images of electrospun nanofiber: F1- PCL nanofiber (8% w/v), F2- PCL nanofiber (12% w/v), F3- PCL/CHL nanofiber, and F4- PCL/CHL/Que nanofiber.

protein, with the unit being the amount of SOD required to inhibit 50% NBT reduction by super-oxide radicals.

The Hydrogen peroxide scavenging activity of catalase in the supernatant was determined by method described by Aebi [24]. The assay is based on the direct measurement of the decrease in absorbance of H_2O_2 (at 240 nm) due to its decomposition by catalase. 0.17 M ethanol (0.01 mL/mL of supernatants) was added in the supernatants to prevent the formation of inactive complex-II (catalase-H_2O_2 complex-II). The reaction mixture was prepared by adding 1 mL H_2O_2 (30 mM in potassium phosphate buffer, pH 7.4) in 2 mL of above supernatants. The reaction was started immediately after addition of H_2O_2. Diminishing UV-absorbance of the sample was recorded at 240 nm for 3 min at intervals of 30 sec. The catalase activity was calculated by the following equation:

$$Catalase\ activity = \left(\frac{2.3}{\Delta t}\right)\left(\frac{a}{b}\right)\left(\log\frac{A_1}{A_2}\right) \quad (6)$$

where, A_1 and A_2 are absorbances of solution at two consecutive time, a is dilution factor, b is protein content (mg/mL), and Δt is time interval i.e. 0.5 min. The catalase activity was expressed as Unit/mg protein, with the unit expressed as mM of H_2O_2 consumed per min.

Hydroxyproline assay

Being a stable parameter of collagen, hydroxyproline level in the tissue can be used as a biochemical marker of collagen metabolism. For Hydroxyproline assay, the procedure was adapted from Reddy and Enwemeka with some modification [25]. Granulated tissues were treated thrice with acetone for 6 h to remove any possible fat. Fat-free samples were acid-hydrolyzed (6 N HCl,

50 mg sample/mL) for 6 h at 120 °C to yield individual amino acid. Hydrolyzed samples were allowed to cool and neutralized with 2 N NaOH solution (phenolphthalein solution). 50 μL of each hydrolyzate was added to 96-well plate and mixed with chloramine-T (450 μL) and incubated for 25 min to form oxidation product, pyrrole-2-carboxylate. In each reaction mixture 500 μL of Ehrlich's solution was added and incubated for 25 min at 65 °C, which resulted in the conversion of pyrrole-2-carboxylate to a chromophore (reddish purple complex). The absorbance of chromophore was measured at 550 nm with a microplate reader. Hydroxyproline content was determined from the standard curve of pure amino acid (10–100 μg/mL).

Statistical analysis

All the experimental results were expressed as mean ± standard deviation (SD) and statistically compared
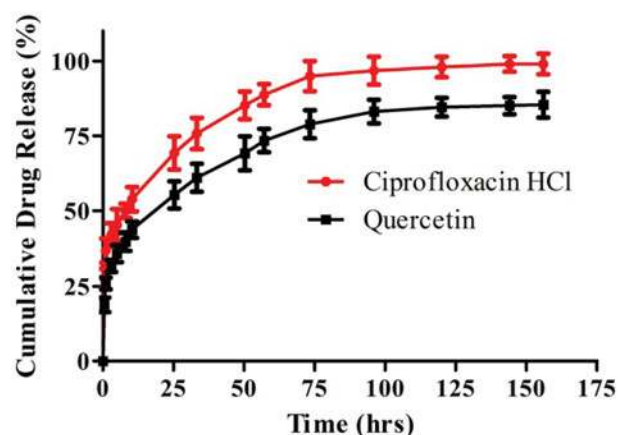

Figure 4. *In-vitro* cumulative drug release profiles of ciprofloxacin HCl and quercetin loaded nanofiber in PBS (pH 7.4). The data are represented as mean ± SD, $n = 3$.
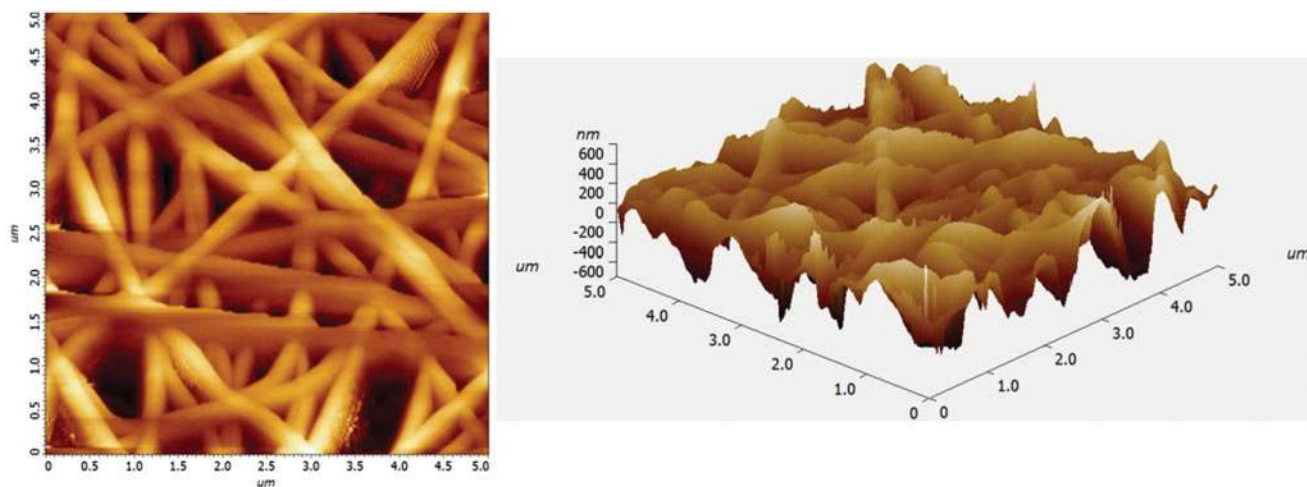

Figure 3. Two dimensional and three dimensional morphology of PCL/CHL/Que nanofiber showing bead-free and continuous nanofiber.

either by one-way ANOVA (Tukey's post-test) or two-way ANOVA (Bonferroni post-tests) using GraphPad Prism (Version 5.01, GraphPad Software). The experimental results with p values $< .05$ were assumed as statistically significant.

Results and discussion

Characterization of nanofiber membrane

Morphological study

PCL based nanofiber of different compositions were successfully electrospun using acetic acid/formic acid solvent system, which are one of the most commonly used solvent compositions for electrospinning. Effect of polymer concentration and drug concentration (CHL and Que) on nanofiber diameter and morphology can be seen in Figure 2. At low polymer concentration (8%w/v) nanofiber formed with a thin diameter (60.35 ± 27.78 nm) and inconsistent morphology, i.e., beading (Figure 2-F1). The plausible reason is insufficient viscosity of the solution which experiences two kinds of instabilities during travel from the nozzle to collector. First one is higher bending instability which results into thin diameter nanofiber [26], another one is Rayleigh instability which results into a beaded structure [27]. As the polymer concentration increased to provide sufficient viscosity, bead-free fibre with thick diameter (79.07 ± 22.49 nm) was obtained (Figure 2-F2). The probable reason is sufficient viscosity solutions which provide higher resistance to the jet against

bending instability and Rayleigh instability. When CHL was added, it results in more continuous nanofiber with little lateral perturbation (Figure 2-F3). CHL incorporation results into enhancing polarity of solution due to HCl salt. This additional charge increases the repulsive forces between adjacent charged molecule carried by jet and result into lateral perturbation [28]. Very few lateral perturbations were observed in PCL/CHL/Que nanofiber which might be due to dilution of charge by addition of Que (Figure 2-F4). Production of more continuous fibre in F3 and F4 might be due to the plasticizing effect of the drugs which increases the spinning ability of the solution. No significant difference had been observed between the diameter of PCL/CHL-nanofiber (126.11 ± 33.57) and PCL/CHL/Que-nanofiber (101.59 ± 29.18).

Porosity of a scaffold becomes an important parameter, when it is intended to be used for skin reconstitution. The porous nature of nanofiber would be helpful for cellular infiltration and proliferation; exchange of exudates, gases, and nutrients across the wounded area. The ideal porosity of scaffolds should usually be

Table 2. 'Time-dependent' DPPH scavenging efficacy of ciprofloxacin HCl and quercetin loaded nanofiber in PBS (pH 7.4).

Incubation Time (h)	DPPH Scavenging Activity (%)
0.5	40.13 ± 3.01
1	47.63 ± 2.34
2	51.09 ± 0.92
4	57.61 ± 1.02
8	62.41 ± 2.98
12	68.20 ± 2.33

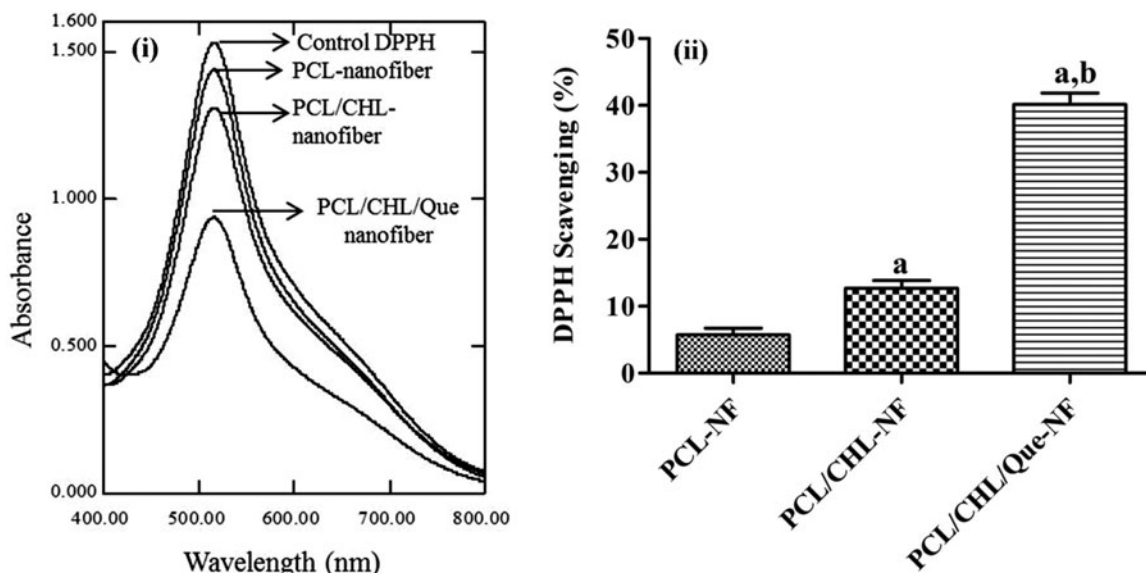Data are represented as mean $\pm$ SD ($n = 3$).

Figure 5. DPPH scavenging activity of nanofiber on 'fixed reaction time': (i) UV-visible spectra of different DPPH solution after 30 min incubation; (ii) bar graph comparing the scavenging efficacies of different nanofiber. [a]$p < .05$ compared to PCL-NF; [b]$p < .05$ compared with PCL/CHL-NF. The data represented as mean $\pm$ SD, $n = 3$.
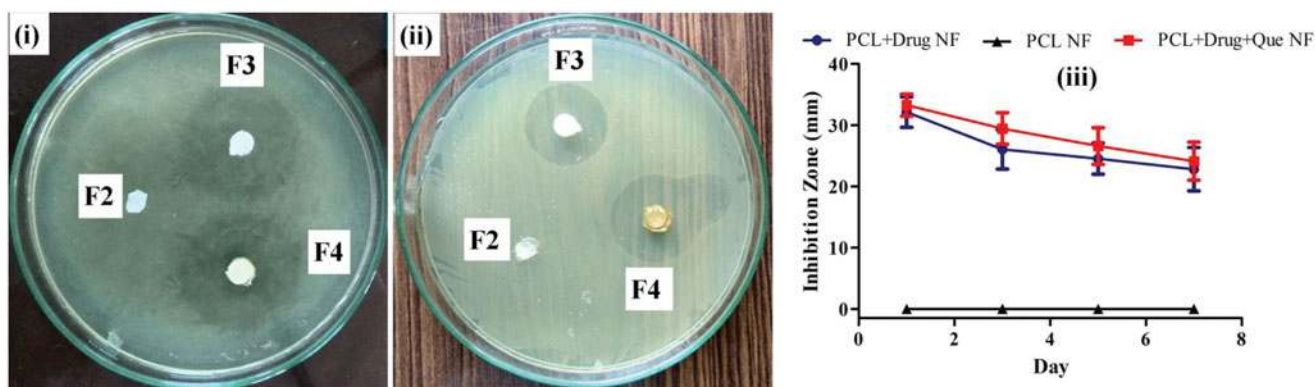
Figure 6. Agar plate showing the growth inhibition zone of *S. aureus* on (i) day 1, and (ii) day 7. F2, F3, and F4 represent PCL, PCL/CHL, and PCL/CHL/Que loaded nanofiber. Graph (iii) outline the relation between inhibition zone (mm) and time (days). The data represented as mean $\pm$ SD, $n = 3$.
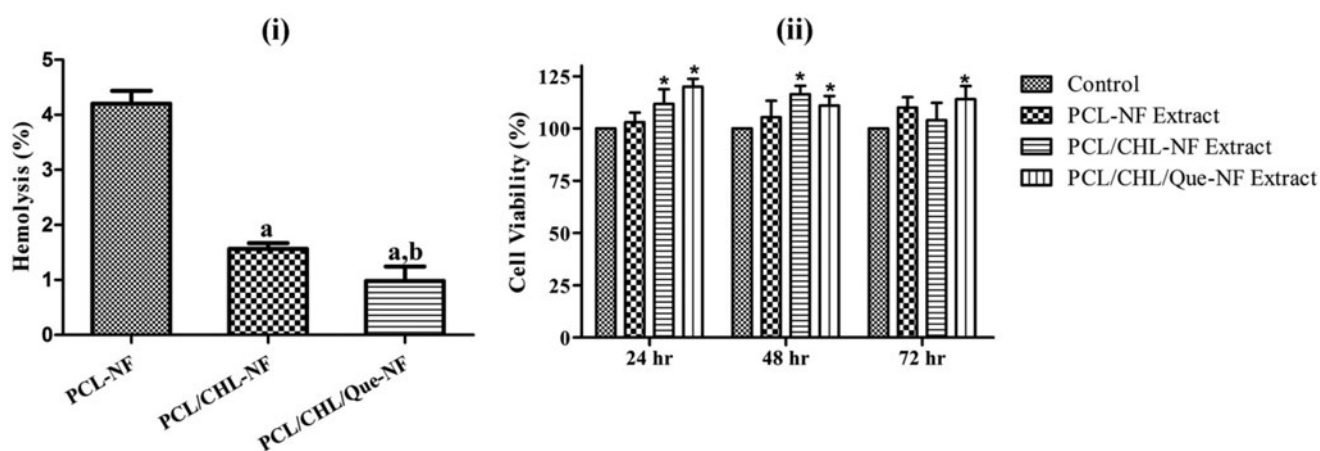

Figure 7. Biocompatibility of fabricated scaffold: (i) haemolysis activity of different nanofiber. [a]$p < .05$ compared to PCL-NF; [b]$p < .05$ compared with PCL/CHL-NF, and (ii) viability of fibroblast cells after treatment with the extract of different nanofiber. *$p < .05$ versus control. The data are represented as mean $\pm$ SD, $n = 3$.

within the range of 60–90% [3]. The developed membranes possessed the optimum porosity (data shown in Table 1) with randomly oriented nanofiber, which closely mimics the natural ECM.

Three dimensional morphological and topographical variation of PCL/CHL/Que nanofiber was studied using atomic force microscopy which was produced after atomic level interaction between scanner tip and surface of nanofiber. The diameter of nanofiber obtained from study was found in agreement to SEM finding. AFM micrographs (Figure 3) displayed bead-free, continuous, and randomly interconnected nanofiber.

Solid-state characterizations

Any possible drugs-excipient interaction and change in crystallinity was studied by FTIR and XRD, respectively. It can be concluded from the results (refer S5 and Figure S1) that drugs were chemically compatible with

PCL and those were entrapped in amorphous form in the nanofiber.

Drug entrapment efficiency and in-vitro release profile

Since only in-situ solidification of the polymer solution takes place in electrospinning, therefore, the entrapment efficiency of a nanofiber film should be almost 100%, under the consideration of complete miscibility of drug and polymer, non-volatile nature of the drug, and optimum concentration of the drug. At higher concentration of the drug, the encapsulation efficiency decreases, most likely due to the loss of excess drug as the aggregate on the nanofiber surface, which escape encapsulation into the nanofibers. The fabricated nanofibers exhibited high entrapment efficiency (Table 1) which might be due to better miscibility of polymer
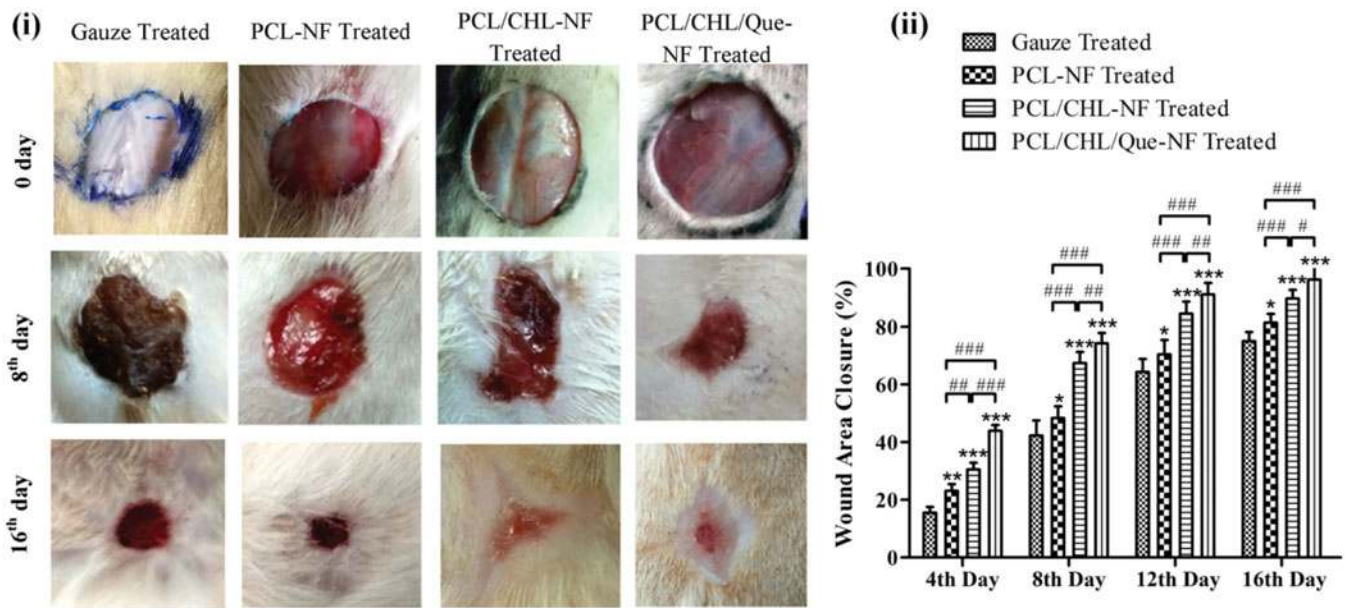
Figure 8. *In-vivo* healing of full thickness wound: (i) images of wounds, and (ii) wound area closure rate after treatment with gauze, PCL, PCL/CHL, PCL/CHL/Que-nanofiber at different time interval. $*p < .05$, $**p < .01$ and $***p < .001$ versus gauze treated group; $^{\#}p < .05$, $^{\#\#}p < .01$ and $^{\#\#\#}p < .001$. The data are expressed as means $\pm$ SD, $n = 6$.
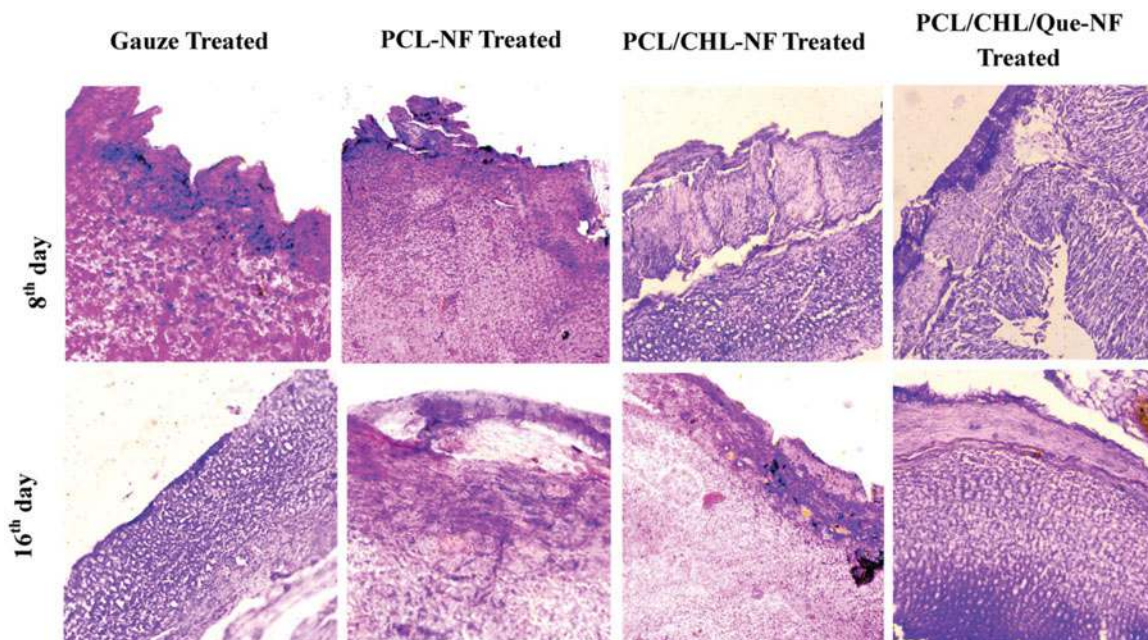
Figure 9. Haematoxylin − eosin stained slice showing histological changes in granulation tissue after treatment with gauze, PCL-NF, PCL/CHL-NF and PCL/CHL/Que-NF.

and drug(s), and negligible loss of drug(s) which is also supported by XRD data.

The *in-vitro* release profiles of PCL/CHL/Que-nanofiber in PBS (pH 7.4) are shown in Figure 4. The release of encapsulated drugs occurred in a biphasic manner, with an initial burst release followed by prolonged release. The initial burst release could be due to leaching of drug molecules located close to the surface of nanofiber membrane which was in immediate contact with dissolution media whilst the prolonged release over longer time might be due to diffusion of the drugs molecules that is lying deeper within the PCL nanofiber. Poor solubility of quercetin at pH 7.4 might be the plausible reason for its low initial burst release (39.78% in 8 h) and cumulative release (85.09% in 6 days) in comparison to ciprofloxacin HCl release.

Figure 10. Biochemical assessment of granulation tissue harvested from wound area in terms of (i) SOD, (ii) catalase activity, and (iii) hydroxyproline content on day 8th and 16th. $*p < 0.05$, $**p < .01$, $***p < .001$, and $^{\$}p > .05$ versus gauze treated group; $^{\#}p < .05$, $^{\#\#}p < .01$, $^{\#\#\#}p < .001$ and $^{ns}p > .05$. The data are expressed as means $\pm$ SD, $n = 6$. Control is an unwounded group.
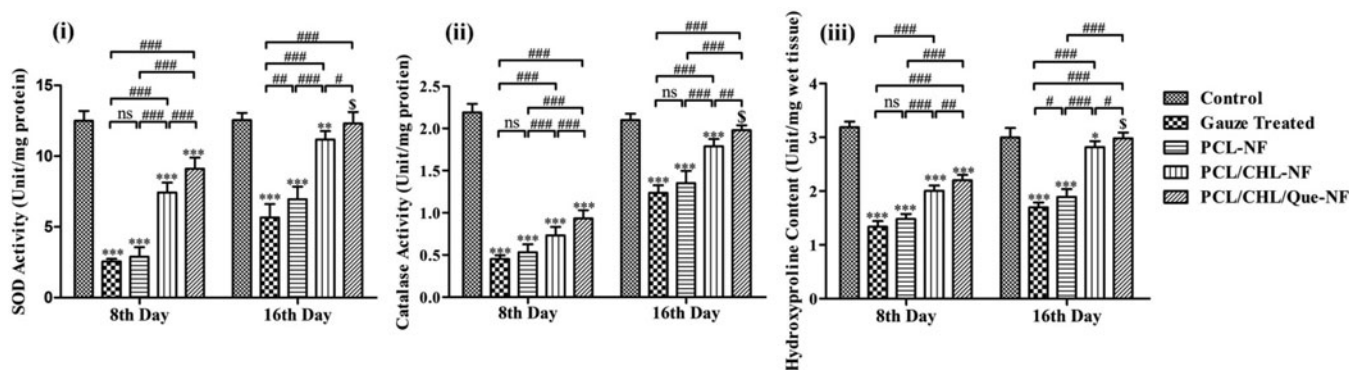
Since the fundamental purpose was to reduce the bacterial infection and attenuation of ROS generated during the early phase of wound healing, the burst release of ciprofloxacin HCl and quercetin was desired and the same was observed in PCL/CHL/Que-nanofiber membrane.

In-vitro *antioxidant activity*

Antioxidant efficacy of the nanofiber film has been examined by DPPH assay and shown in Figure 5. The fundamental principle behind this assay is that DPPH is a stable free radical with maximum absorbance at 517 nm and it changes its colour from purple to yellow on accepting a hydrogen (H) or an electron from the antioxidant (like quercetin) and is reduced itself to $DPPH_2$. The colour change is measured by UV-spectrophotometer at 517 nm and utilized for quantification of antioxidant concentration in the solution [19]. It was found that PCL nanofiber and PCL/CHL-nanofiber also exhibited slight antioxidant activity, 5.75%, and 12.67% respectively, which might be due to terminal hydroxyl group in PCL and hydroxyl group in ciprofloxacin. PCL/CHL/Que-nanofiber exhibited quite significant ($p < .001$) anti-oxidant property (40.13%), which was because of phenolic groups in quercetin. Table 2 shows the variation in DPPH scavenging efficiency of ciprofloxacin HCl and quercetin loaded nanofiber with respect to different time interval. It is found that DPPH scavenging activity increases with incubation time, which is due to the fact that with increase in incubation time the amount of quercetin released also increases, which results into increasing scavenging of DPPH.

In-vitro *antibacterial activity*

The antimicrobial activity of fabricated nanofibers was tested against *S. aureus* by using film diffusion method and shown in Figure 6. Placebo nanofiber exhibits no antimicrobial property at all times. In contrast, PCL/CHL and PCL/CHL/Que-nanofiber displayed initially broad inhibition zone due to burst release of antimicrobial; later these nanofibers showed sustained antimicrobial activity. PCL/CHL/Que-nanofiber exhibited a little wide inhibition zone than PCL/CHL nanofiber, although no significant difference between PCL/CHL and PCL/CHL/Que-nanofiber antimicrobial activity had been observed at any time. Therefore, it can be concluded that electrospun film was active enough to prevent microbial growth during the study period and antimicrobial activity of loaded CHL in nanofiber was not altered due to electrospinning.

Biocompatibility assay

Hemocompatibility of nanofiber membrane

Hemo-compatibility of a scaffold proposed to be used in wound area is a vital requirement to maintain the integrity and functionality of RBCs in newly formed blood capillaries else it may cause some serious concern like thrombosis. International standard allows ~1% spontaneous haemolysis limit [20]. Accordingly, hemo-compatibility of nanofiber Film was evaluated by measuring the haemolytic property on human RBCs. The extent of RBCs haemolysis by electrospun nanofibers are shown in Figure 7 (a). It was observed that placebo nanofiber caused $4.20 \pm 0.23\%$ haemolysis which might be due to high surface roughness of the film. Although, the haemolytic value of PCL/CHL and PCL/

CHL/Que nanofiber is close to the acceptable limit, a significant ($p < .05$) difference between their values was observed, which might be due to protective action of quercetin against lipid peroxidation of unsaturated fatty acid and thiol group (-SH) in RBCs membrane.

Cytocompatibility of nanofiber membrane

The Viability of fibroblast cell lines on 24 h, 48 h, and 72 h was examined through MTT assay and shown in Figure 7 (b). It was observed that the cell lines proliferated well in all aliquots throughout the study period, which confirm the nontoxic nature of nanofibers. At the end of each time point, cell lines treated with PCL/CHL/Que-nanofiber's aliquot showed significant ($p < .05$) proliferation, which might be due to quercetin, a flavonoid. Flavonoids are found to improve the fibroblast proliferation and collagen synthesis [8].

In-vivo wound healing study

All the four groups showed no post-operative side effect like sepsis, fluid retention, etc. throughout the treatment period and nanofiber scaffold adhered well on the wound site. It can be observed from Figure 8 that among all treatment groups, PCL/CHL/Que-nanofiber treated group exhibited superior wound healing property at all-time point. At the end of 4th day, PCL/CHL/Que-treated group displayed significant ($p < .001$) healing (43.98%) in comparison to PCL/CHL treated group (30.56%), which might be due to effective attenuation of ROS during inflammatory phase by burst released of quercetin. During proliferation and maturation phase, PCL/CHL/Que group still showed significant wound contraction but of the varying level ($p < .01$ and $p < .05$ on the 12th day and 16th day, respectively). Throughout the study period, PCL/CHL and PCL/CHL/Que group maintained a significant ($p < .001$) wound healing efficiency with respect to gauze and PCL-nanofiber treated group. Antimicrobial and antioxidant property of nanofiber might have reduced microbial infection, ROS level and prevented the oxidative damage of fibroblast, thereby improving the collagen synthesis and wound healing potential.

Histological examination

The histological sections of H&E stained skin of gauze treated and scaffold treated groups on days 8 and 16 are shown in Figure 9. On day 8, underplaying layer of granulated tissue of gauze treated group was infiltrated with inflammatory cells like neutrophils and basophils. Wounds in PCL nanofiber treated group displayed the granulation tissue with fewer fibroblasts along with neutrophils and macrophages. Groups

treated with PCL/CHL and PCL/CHL/Que-nanofiber demonstrated moderate amount of fibroblast as compared to the other groups, which confirm the accelerated wound healing. Inflammatory response is very low in PCL/CHL/Que treated group, establishing the anti-oxidant activity of quercetin. All four groups displayed moderate amount of blood capillaries.

On day 16, gauze treated group shows incomplete re-epithelialization and PCL nanofiber treated group showed moderate epithelialization along with thin epidermis. Both groups displayed poor collagen synthesis as white spaces in dermis region. On the other side, PCL/CHL and PCL/CHL/Que nanofiber treated groups exhibited well developed epidermis and dermis layer along with keratinocyte infiltration and good collagen deposition in epidermis and dermis layer respectively.

Antioxidant enzyme assay

In the excision wound model, the inflammatory phase generally spans for 1–4 days, during which ROS generated beyond the physiological need [7]. During this phase, endogenous anti-oxidants become insufficient to attenuate this excess ROS. Even exogenous anti-oxidant (like Quercetin) did not restore the activity of endogenous enzymes significantly in the first week of study, which could be observed in Figure 10 (a,b). At the end of first week none of the groups exhibited significant improvement in the amount of SOD and catalase. Although PCL/CHL/Que-nanofiber treated animals demonstrated significant ($p < .001$) improvement in anti-oxidants level in comparison to other groups, which could be due to potential anti-oxidant property of quercetin, but still did not cause insignificant difference with respect to control. During proliferative phase (5–11 days), only a small amount of ROS were generated which could be attenuated by collective effect of extracellular and intracellular anti-oxidants. Therefore, during those phases extracellular antioxidant helped in restoration of SOD and catalase level, as observed at the end 16th day. Quercetin loaded nanofiber group had achieved SOD and catalase level very close to control ($p > .05$) and meanwhile it also achieved a significant ($p < .05$) improvement in antioxidants level when compared with rest treated groups.

Hydroxyproline assay

Granulation tissue is mainly constituted of collagen fibre, fibroblast and newly developed blood vessel. Collagen fibre is composed of 13–14% hydroxyproline in addition to other amino acid. Hence, hydroxyproline

level has been used as biochemical index for collagen content. The content of hydroxyproline or collagen fibre indicates activity of proliferating fibroblast and physical strength of regenerating tissue. On the 8th day, all groups demonstrated insignificant ($p < .001$) improvement in comparison with control, although PCL/CHL-nanofiber and PCL/CHL/Que-nanofiber treated groups displayed significant improvement ($p < .001$) in comparison to rest two groups (Figure 10(c)). This increment could be attributed to pro-wound healing environment provided by nanofiber. On the 16th day, only PCL/CHL/Que-nanofiber treated group showed significant increase in hydroxyproline level in respect to other groups. Although hydroxyproline level was higher in PCL/CHL-nanofiber treated group than in the gauze treated and PCL-nanofiber group, but no significant difference could be achieved between PCL/CHL-nanofiber treated group and control. On both time points, PCL/CHL/Que-nanofiber treated animals exhibited significant ($p < .05$) improvement in wound healing in respect of PCL/CHL-nanofiber treated group, which could be due to neutralization of reactive oxygen species and subsequently better collagenases.

Conclusions

In this study, a scaffold having potential antimicrobial and antioxidant property was electrospun successfully by incorporating ciprofloxacin HCl and quercetin in PCL nanofiber. The fabricated membrane possessed bead-free, continuous nanofiber with a narrow diameter and optimum porosity which was able to support cellular infiltration and proliferation. PCL/CHL/Que-nanofiber was quite effective to inhibit bacterial load and excess free radicals activity in wound area by releasing the drugs in a biphasic manner. Further, the antimicrobial and antioxidant activity of the scaffold was established by screening against *S. aureus* seeded on an agar plate and DPPH scavenging activity, respectively. Quercetin loaded nanofiber was able to preserve the functionality of RBCs by protecting it against lipid peroxidation. Similarly, it maintained the fibroblast viability by shielding it against oxidative damage. Thus, the developed nanofiber proved its hemocompatibility and cytocompatibility activity. Further, *in-vivo* healing of full thickness wound demonstrated that PCL/CHL/Que-nanofiber has significantly good wound healing property. This result was further corroborated by biochemical analysis of granulation tissue, which showed that scaffold had effectively restored the SOD, catalase and

hydroxyproline level. Conclusively, this study endorses the use of PCL based nanofiber loaded with ciprofloxacin HCl and quercetin as better wound healing dressing material.

ORCID

Gufran Ajmal http://orcid.org/0000-0001-8576-2386
Gunjan Vasant Bonde http://orcid.org/0000-0002-4252-0966
Sathish Thokala http://orcid.org/0000-0002-0380-1140
Pooja Mittal http://orcid.org/0000-0001-7961-6964
Juhi Singh http://orcid.org/0000-0002-6071-3307
Brahmeshwar Mishra http://orcid.org/0000-0002-8608-2611

References

[1] Kant V, Jangir BL, Nigam A, et al. Dose regulated cutaneous wound healing potential of quercetin in male rats. Wound Med. 2017;19:82–87.

[2] Gautam S, Dinda AK, Mishra NC. Fabrication and characterization of PCL/gelatin composite nanofibrous scaffold for tissue engineering applications by electrospinning method. Materials Sci Eng C. 2013;33:1228–1235.

[3] Chong E, Phan T, Lim I, et al. Evaluation of electrospun PCL/gelatin nanofibrous scaffold for wound healing and layered dermal reconstitution. Acta Biomater. 2007;3: 321–330.

[4] Norouzi M, Shabani I, Ahvaz HH, et al. PLGA/gelatin hybrid nanofibrous scaffolds encapsulating EGF for skin regeneration. J Biomed Mater Res. 2015;103:2225–2235.

[5] Liu S-J, Kau Y-C, Chou C-Y, et al. Electrospun PLGA/collagen nanofibrous membrane as early-stage wound dressing. J Membrane Sci. 2010;355:53–59.

[6] Ma K, Liao S, He L, et al. Effects of nanofiber/stem cell composite on wound healing in acute full-thickness skin wounds. Tissue Eng Part A. 2011;17:1413–1424.

[7] Nafiu AB, Rahman MT. Anti-inflammatory and antioxidant properties of unripe papaya extract in an excision wound model. Pharm Biol. 2015;53:662–671.

[8] Selvaraj S, Fathima NN. Fenugreek incorporated silk fibroin nanofibers- a potential antioxidant scaffold for enhanced wound healing. ACS Appl Mater Interfaces. 2017;9:5916–5926.

[9]   Xue J, He M, Liang Y, et al. Fabrication and evaluation of electrospun PCL–gelatin micro-/nanofiber membranes for anti-infective GTR implants. J Materials Chem B. 2014;2: 6867–6877.

[10] Celebioglu A, Umu OC, Tekinay T, et al. Antibacterial electrospun nanofibers from triclosan/cyclodextrin inclusion complexes. Colloids Surf B Biointerfaces. 2014;116: 612–619.

[11] Xue J, He M, Liu H, et al. Drug loaded homogeneous electrospun PCL/gelatin hybrid nanofiber structures for anti-infective tissue regeneration membranes. Biomaterials. 2014;35:9395–9405.

[12] Kim SE, Heo DN, Lee JB, et al. Electrospun gelatin/polyurethane blended nanofibers for wound healing. Biomed Mater. 2009;4:044106.

[13] Kevadiya BD, Rajkumar S, Bajaj HC, et al. Biodegradable gelatin–ciprofloxacin–montmorillonite composite hydrogels for controlled drug release and wound dressing application. Colloids Surf B Biointerfaces. 2014;122: 175–183.

[14] Unnithan AR, Barakat NA, Pichiah PT, et al. Wound-dressing materials with antibacterial activity from electrospun polyurethane–dextran nanofiber mats containing ciprofloxacin HCl. Carbohydr Polym. 2012;90:1786–1793.

[15] Jannesari M, Varshosaz J, Morshed M, et al. Composite poly (vinyl alcohol)/poly (vinyl acetate) electrospun nanofibrous mats as a novel wound dressing matrix for controlled release of drugs. Int J Nanomed. 2011;6:993–1003.

[16] Li Y, Yao J, Han C, et al. Quercetin, inflammation and immunity. Nutrients. 2016;8:167

[17] Arvand M, Tajyani S, Ghodsi N. Electrodeposition of quercetin on the electrospun zinc oxide nanofibers and its application as a sensing platform for uric acid. Mater Sci Eng C Mater Biol Appl. 2015;46:325–332.

[18] Aceituno-Medina M, Mendoza S, Rodríguez BA, et al. Improved antioxidant capacity of quercetin and ferulic acid during in-vitro digestion through encapsulation within food-grade electrospun fibers. J Function Foods. 2015;12:332–341.

[19] Mishra K, Ojha H, Chaudhury NK. Estimation of antiradical properties of antioxidants using DPPH assay: a critical review and results. Food Chem. 2012;130:1036–1043.

[20] Vijayakumar MR, Kumari L, Patel KK, et al. Intravenous administration of trans-resveratrol-loaded TPGS-coated solid lipid nanoparticles for prolonged systemic circulation, passive brain targeting and improved in vitro cytotoxicity against C6 glioma cell lines. RSC Adv. 2016;6: 50336–50348.

[21] El-Ferjani RM, Ahmad M, Dhiyaaldeen SM, et al. In vivo assessment of antioxidant and wound healing improvement of a new schiff base derived co (II) complex in rats. Sci Rep. 2016;6:38748

[22] Beauchamp C, Fridovich I. Superoxide dismutase: improved assays and an assay applicable to acrylamide gels. Anal Biochem. 1971;44:276–287.

[23] Ak T, Gülçin İ. Antioxidant and radical scavenging properties of curcumin. Chem Biol Interact. 2008;174:27–37.

[24] Aebi H. [13] Catalase in vitro. Meth Enzymol. 1984;105: 121–126. Vol. Elsevier;

[25] Reddy GK, Enwemeka CS. A simplified method for the analysis of hydroxyproline in biological tissues. Clin Biochem. 1996;29:225–229.

[26] Khan G, Patel RR, Yadav SK, et al. Development, optimization and evaluation of tinidazole functionalized electrospun poly (ε-caprolactone) nanofiber membranes for the treatment of periodontitis. RSC Adv. 2016;6: 100214–100229.

[27] Rieger KA, Birch NP, Schiffman JD. Designing electrospun nanofiber mats to promote wound healing–a review. J Mater Chem B. 2013;1:4531–4541.

[28] Reneker DH, Yarin AL, Fong H, et al. Bending instability of electrically charged liquid jets of polymer solutions in electrospinning. J Appl Phys. 2000;87:4531–4547.